land

MDPI

Article

Predicting Urban Expansion to Assess the Change of Landscape Character Types and Its Driving Factors in the Mountain City

Jinsen Mou [1], Zhaofang Chen [2,*] and Junda Huang [2]

[1] Shanghai Garden (Group) Ltd., Shanghai 200092, China; sggchr@163.com
[2] Department of Landscape Architecture, College of Architecture and Urban Planning, Tongji University, Shanghai 200092, China; jundahuang1991@gmail.com
* Correspondence: 1910238@tongji.edu.cn

Abstract: The urban landscape is being affected by rapid urbanization, leading to a complexity of land features and a fragmentation of patches. However, many studies have focused on the prediction of land-use change with a lack of research on the landscape character types which have more integrated descriptions of land features. Hence, this study predicts and identifies landscape character types (LCTs) in different periods based on the PLUS model and the K-Medoids algorithm, taking the central city of Chongqing as an example, to reveal the differences in the influence of driving factors on LCTs. The results show that (1) the urban landscape characteristic types present a gradient change from the built-up area to the outward expansion. (2) The SHDI and LPI of landscape character types decreased significantly with the expansion of construction land. (3) Nighttime light, distance from water bodies, and distance from the motorways are the main factors affecting the change of landscape character types. This study predicts and identifies urban landscape character types and quantifies the impact of urban expansion on landscape character. It can be used to guide urban planning and help governments to make more informed decisions on sustainable urban development and ecological conservation.

Keywords: land-use change; the PLUS model; K-medoids cluster; landscape management

Citation: Mou, J.; Chen, Z.; Huang, J. Predicting Urban Expansion to Assess the Change of Landscape Character Types and Its Driving Factors in the Mountain City. *Land* **2023**, *12*, 928. https://doi.org/10.3390/land12040928

Academic Editor: Rui Alexandre Castanho

Received: 19 March 2023
Revised: 14 April 2023
Accepted: 18 April 2023
Published: 21 April 2023

1. Introduction

Over the past few decades, urbanization has become the dominant process of global environmental change [1]. As land resources on the Earth's surface are finite, the rapid growth of construction land has had a tremendous negative impact on natural ecosystems, biodiversity, and ecological integrity [2,3]. Thus, to ensure sustainable urban development, the analysis of urban expansion patterns has been a hot topic in the current land-use/land cover change research [4,5]. As a vehicle for visualizing the complex interactions between natural factors and human activities in the ecological environment, the land-use/land cover change has profound implications for terrestrial ecosystems, global biodiversity, and regional ecological security [6–9], as well as causing a range of environmental and social problems in local land systems. Especially in mountainous cities, undulating hills and winding rivers divide the whole region into diverse landscape spaces, resulting in a significant and complex impact on urban expansion [10–12]. Therefore, simulating and predicting urban expansion patterns has become key to ecosystem protection and sustainable development [13], providing insight into the environmental impacts of human activities.

Among the many methods for modeling and predicting urban expansion patterns, land-use change simulation is one of the most commonly used tools for urban land change analysis, allowing planners to visualize potential land-use changes through different scenarios [14]. The urban expansion scenario based on the land-use change simulation has been widely studied in many fields, such as ecology and climatology. For example, Yan Zhang et al. used the cellular automata (CA)–Markov model to predict land-use for an

ecologically constrained urban sprawl simulation in Wuhan, China [15]. Onuwa Okwuashi et al. presented a novel integration of a support vector machine, Markov chain, and cellular automata for urban change modeling in Nigeria, Africa's most populous city [16]. In Paris, A. Lemonsu et al. employed a land-use–transport interaction, socio-economic model, and an urban climate model to simulate urban temperatures under five urban expansion scenarios [17]. There is also a study that used the Multi-layer perceptron (MLP)-based Artificial Neural Network–Markov Chain (ANN-Markov) model to simulate three future urban growth scenarios in Miami's Metropolitan Area. It assesses the future flood risk under each scenario [18].

However, the majority of past research has focused on the relationship between land-use and urban expansion, ignoring the complex impacts of land-use change on urban landscapes. Changes in landscape patterns can interfere with important ecological processes [19]. Therefore, the lack of research on urban landscape patterns is a barrier to the planning of sound interventions by city managers and the maintenance of the results of the guidelines [20,21].

Landscape character is a common means of describing the spatial variability of a landscape pattern. It is defined as a unique and identifiable pattern of elements that occur repeatedly across a given landscape type [22]. A particular combination of the natural landscape components (topography, soils, vegetation) and the man-made landscape components (built-up areas, villages) create landscape characters that distinguish one landscape from another, generate different perceptible characteristics, and make an area unique [23]. Landscape Character Appraisal was one of the first tools proposed by the Countryside Agency in England to investigate, analyze, evaluate, and propose sustainable development decisions for landscapes at a range of scales, from national to local [24]. Through constructing indicator systems, researchers can identify the most prominent landscape characters in a region to guide urban management [25].

Typically, urban landscape characters are described in terms of landform, function, and transportation [26]. Multi-dimensional characteristics such as topography, land-use, vegetation cover, population, culture, and ecosystem services are used to assess and classify urban and rural landscape characters on a larger scale [27]. However, most existing studies focus on assessing and classifying the current state of landscape characters, and little attention has been paid to changes in their types. Changes in the landscape character type (LCT) can have an impact on ecological processes and lead to variations in the level of ecosystem services and landscape perception [19]. Therefore, the monitoring and prediction of changes in LCTs will be useful in the management of the environmental risks that may be associated with urban expansion [28].

Therefore, this study optimized the methodology of existing studies, emphasizing the modularity of indicator selection and the calculation process of landscape characters. Chongqing, a typical mountain city with rich landscape characters, was chosen as the study area. The natural environment, society and economy, and transport were used to predict future land-use. A framework for identifying LCTs based on land-use prediction was constructed for decision-makers by clustering LCTs in the topography, landscape pattern, and land-use. This study answered three main questions: (1) What are the major changes in LCTs during urban expansion? (2) How does the composite index system affect LCT change? (3) What are the driving factors that influence the changes in land-use and the LCTs? From a regional scale perspective, this study focuses on built-up areas and can be considered as a guide for future landscape character analysis/urban planning in mountainous cities.

2. Study Area and Data

2.1. Study Area

Chongqing (105°11′~110°11′ E, 28°10′~32°13′ N) is located in the interior of southwest China, with a landscape dominated by hills and mountains. The terrain slopes gradually from north–south to the Yangtze River. There are four parallel mountains running north–

south (Jinyun, Zhongliang, Tongluo and Mingyue). Two rivers run from east–west (Jialing River and Yangtze River) [29]. Chongqing has 38 districts and counties and, according to data from 2020, a population of 10.34 million [30]. Aside from being an important central city in western China, Chongqing is also a comprehensive transportation hub of the Yangtze River economy belt, with unique location benefits [31].

In recent years, rapid urbanization has led to the encroachment of construction land into the natural environment and countryside in Chongqing, which has become a typically frequented region for the study of mountain city development and landscape character change [32]. Simultaneously, the environment of "two rivers and four mountains" means the development of built-up areas is affected by the multiple influences of natural resources, traffic arrangements, and human activities. A series of localized environmental protection policies have forced the countryside to undergo rapid land-use change and ecological degradation compared to built-up areas. All these imply a complex spatial relationship between urban expansion and landscape character.

The central city of Chongqing was selected as the study area, including the Yuzhong (YZ) District, Yubei (YB) District, Jiangbei (JB) District, Shapingba (SPB) District, Nan'an (NA) District, Beibei (BB) District, Jiulongpo (JLP) District, Dadukou (DDK) District, Banan (BN) District, and Bishan (BS) District, with mountains, plains, and hills, with a total area of 6380.62 km^2 (Figure 1).

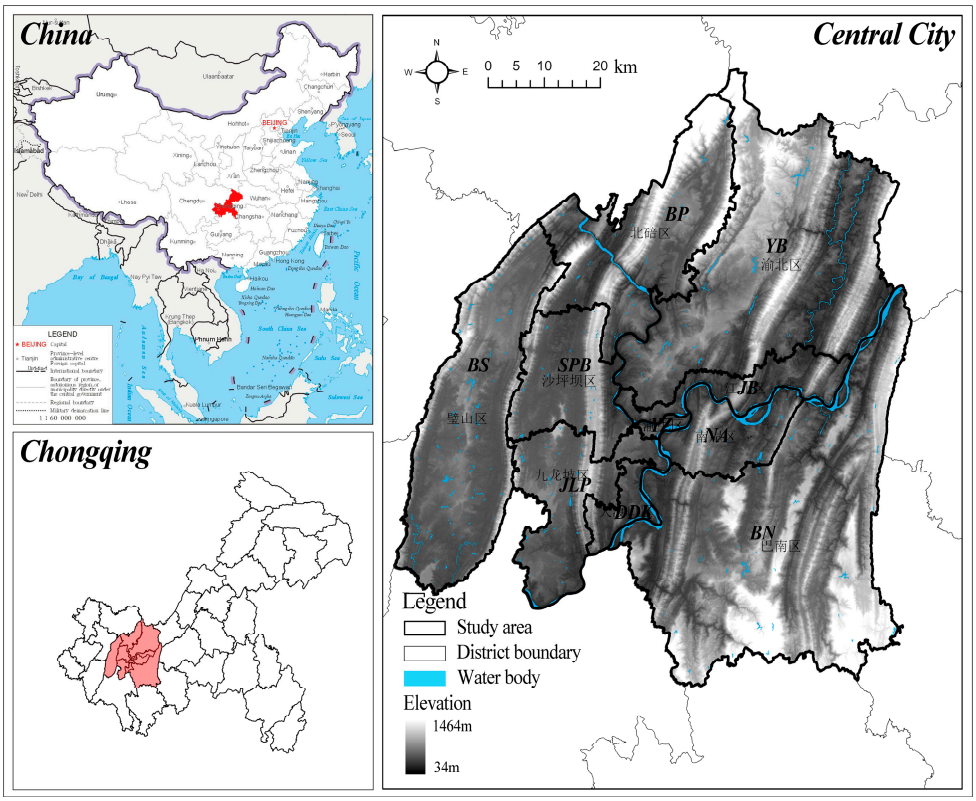

Figure 1. Study area.

2.2. Data and Pre-Precession

A total of five types of data were used in this study, including the land-use, the digital elevation model (DEM), transportation, the Point of Interest (POI), and the socio-economic data (Table 1). The land-use of the study area was obtained from the Resource and Environmental Sciences and Data Center. It was classified into six categories: farmland, forest, grassland, water body, construction land, and other land, according to the landscape characters and study objectives of the study area.

DEM data were obtained from the geospatial data cloud. Elevations and slopes were obtained by processing DEM data with ArcGIS Pro. Transportation data was taken from an Open Street Map (OSM) with vector data of railway, highway, and trunk extracted. POI data were obtained from a Baidu Map, and was used to characterize the functional density of the city.

The socio-economic data included nighttime lights and population density. In this study, nighttime light data published by Chen et al. (2021) were selected, which was based on an algorithm to unify the Defense Meteorological Satellite Program's Operational Linescan System (DMSP/OLS) data from 1992–2013 and National Polar-orbiting Partnership's Visible Infrared Imaging Radiometer (NPP/VIIRS) data after 2013 [33]. Population density data were downloaded from the WorldPop hub. The units are the number of people per square kilometer. The utilized mapping approach was Random Forest-based dasymetric redistribution.

Table 1. Data details.

Data	Source	Format	Year	Resolution
Land-use	www.dsac.cn, accessed on 8 February 2023.	Raster	2000, 2020	30 × 30 m
DEM	www.gscloud.cn, accessed on 8 February 2023.	Raster	— —	30 × 30 m
Transportation	openstreetmap.org, accessed on 8 February 2023.	Vector	2020	— —
Nighttime light	www.nature.com/articles/s41597-022-01322-5, accessed on 8 February 2023.	Raster	2020	1 × 1 km
Population density	www.worldpop.org/, accessed on 8 February 2023.	Raster	2020	30 × 30 arc (approximately 1 km at the equator)
Point of Interests	Baidu map	Vector	2020	— —

To facilitate calculations, the resolution of all data was resampled to 30 × 30 m. The data were also dimensionless by polarization standardization, the equation was: $x' = (x - x_{min})/(x_{max} - x_{min})$. Then, a 1.5 × 1.5 km fishing net was created by ArcGIS Pro, and each square fishing net space represented a study unit.

3. Methodology

To achieve the study objectives, this study includes three steps: firstly, investigating and simulating the changes in land-use in the study area; secondly, identifying and analyzing the LCTs and their changes; and thirdly, exploring the driving factors behind these changes (Figure 2). The simulation and analysis of land-use changes are based on the PLUS model, while the LCTs are objectively classified with an unsupervised clustering approach by constructing an index system to enhance the cognitive understanding of the landscape in the study area.

3.1. Prediction of Land-Use Change

3.1.1. Plus Model

The patch-generating land-use simulation (PLUS) model is an enhanced CA model that integrates the CA model of the multi-type random patch seeds (CARS) and a rule mining approach based on land expansion analysis strategy (LEAS) [34]. This rule mining approach retains the model's ability to analyze the mechanisms of land-use change over time while avoiding the analysis of conversion types, and the issue of exponential growth in the number of categories associated with transformation types [35].

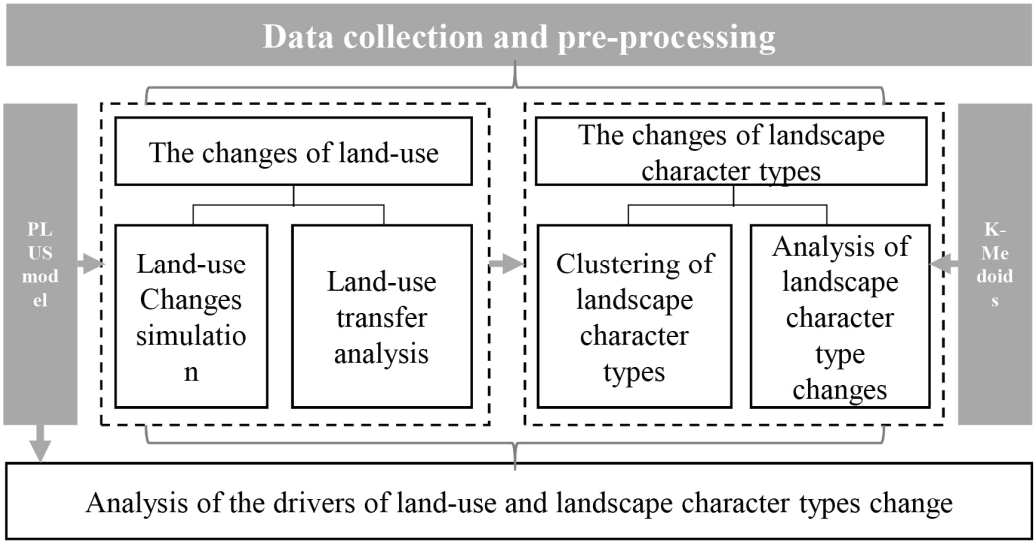

Figure 2. Research framework.

First, the PLUS model extracted land-use expansions for two periods. A random forest algorithm was used to identify the relationship between land-use type change and the different driving forces. LEAS was then used to calculate the probability of growth for each land-use type in the study area. This approach avoids the issue of exponential growth in the number of categories associated with transformation types and retains the model's ability to analyze the mechanism of land-use change during this period while providing improved explanatory power. The number of grids for different land-use types, the conversion matrix, and the neighborhood weights of land-use types were combined to predict the future demand of land-use types via a Markov model. Finally, the future land-use was simulated based on CARS. The CARS module in the PLUS model is a Cellular Automaton (CA) model that incorporates a patch generation mechanism based on various types of random land-use seeds. Throughout the simulation process, the spatial competition for each land-use type is determined by adaptive coefficients, thus driving the expansion to meet the anticipated future demand. The CARS module combines random seed generation and threshold decline mechanisms to enable the PLUS model to dynamically simulate the automatic generation of patches within the bounds of the development probability constraint [36].

3.1.2. Driving Factors Selection

A variety of natural and urban driving factors are the dominant causes of change in land-use types and patterns. Based on the current environment, development plans, and research on driving factors in the central city of Chongqing, this study selected three main categories of driving factors [19,37].

Natural factors represent the strengths and weaknesses of the regional ecological environment. Population concentration and economic development are facilitated by a suitable environment. Chongqing is located in the transition zone between the Tibetan Plateau and the Yangtze River plain [38]. The fact that 76% of the territory is hilly means that not only do the altitudes and slopes have a complex variation but also that the sufficient water resources (lakes and rivers), combined with the hills, divide the city into several areas with different landscape characters. Thus, the conventional factors of mean elevation value, mean slope value, and distance to water bodies were added.

Socio-economic factors play a crucial role in driving the expansion of construction land and investment in sustainable land management [39]. As the urban economy grows and higher demands are placed on the living environment, the population and the Gross Domestic Product (GDP) are beginning to converge [40]. However, rapid urban development is often accompanied by inequitable economic, spatial, and social problems within

cities [41]. The most notable phenomenon in the city of Chongqing is the price of real estate. Influenced by rapid urbanization and Chongqing's natural environment [42,43], large numbers of migrants are moving into the city. The conflict between limited land supply and growing demand has led to a steady rise in urban property prices. High prices are accompanied by a good provision of infrastructure in the surrounding area [44]. Therefore, population density, points of interest (POI) density, and the nighttime light were selected as socio-economic factors influencing land-use change.

Transport accessibility also has a significant impact on land-use change. It is a good indicator of the level of economic development in the area. Local transport accessibility affects the efficiency of intra-city commuting, and regional accessibility influences the price of residences, which means that both have a direct or indirect impact on the development of the regional economy [45]. Convenient transport also has a radiating effect on the economic level of the surrounding areas, which are otherwise congested [46]. Therefore, this study selects the distance to trunk roads, motorways, and primary roads as transport accessibility factors.

3.1.3. Model Parameter Setting

We simulated land-use distribution in 2020 using the CARS module in PLUS v1.3.5, based on the 2000 land-use data and the raster dataset of land-use development probability. The simulated 2020 land-use data were compared to the actual data, and the accuracy of the model was evaluated using the Kappa statistical tool. We conducted multiple tests to obtain optimal parameter settings, ensuring the stability and accuracy of the model.

In this study, patch generation refers to the attenuation coefficient of the decreasing threshold. It was set to 0.2, with a parameter range of 0 to 1, and values closer to 1 corresponded with a higher difficulty of land-use change. Expansion coefficient refers to the probability of random patch seeds. It was set to 0.7, with a parameter range of 0 to 1, and values closer to 1 corresponded with a higher probability of generating new patches. Neighborhood weights refers to the influence of pixels on neighborhood, with a parameter range of 0 to 1, higher values indicated a greater effect on neighborhood. Each neighborhood weight could be calculated by the ratio of the change area of this type to the total change area. Land-use conversion does not usually involve large-scale changes in construction land [47]. Water bodies are also less likely to be converted to other land-uses, as they are protected by strict policies [48]. The development pattern of the study area and the proportion of changes in each land-use type are listed in Table 2.

Table 2. Neighborhood weights of land-use types.

Land-Use Types	Farmlands	Forests	Grasslands	Water Bodies	Urban Construction Lands	Rural Construction Lands	Other Lands
Neighborhood weights	0.15	0.1	0.01	0.03	0.45	0.25	0.01

3.2. Index Systems to Cluster Landscape Character Types

In this study, an index system was constructed to describe the landscape characters of Chongqing city in three dimensions: topography, landscape pattern, and land-use features, aiming to portray the landscape characteristics comprehensively while reducing redundancy. Unlike most large Chinese cities with flat topography, Chongqing has a highly undulating terrain with rivers that run through the city. The relatively flat areas along the river provide areas for urban expansion. Therefore, we selected elevation, slope, and distance to water to characterize the above geographical features. The topography may influence the expansion patterns of construction areas, and landscape pattern indexes can reveal the ecological risks brought about by urbanization through characterizing the morphology and structural features of ecological patches. Thus, the LPI, AWMPED, and

SHDI were selected to describe the landscape pattern characteristics from three aspects: dominance, regularity, and diversity. The land-use indexes were determined by the dominant land-use types. In the study area, urban and rural construction lands, forests, and farmlands play dominant roles, while water bodies and grasslands only account for only 2.79% and 0.71%, respectively. To avoid having too many units with indicator values of 0 (no water bodies or grasslands), we adopted the "distance to water" index to describe the spatial distribution of water bodies. Additionally, grasslands were combined with forests because they are spatially interlaced and can be treated as a whole. The specific indexes and their definitions are shown in Table 3.

Table 3. Details of the index system to cluster LCTs.

Dimension	Indexes	Explanation
Topography	Mean Elevation Value (MEV)	The mean elevation of each unit, used to describe whether it is in a plain, mountainous area, or a transitional zone.
	Mean Slope Value (MSV)	The mean slope of each unit, used to describe whether its terrain is gentle or steep.
	Distance to Water bodies (DW)	The distance of each unit to the water, can reflect the spatial relationship between the samples and the rivers.
Landscape pattern	Largest patch index (LPI)	To calculate whether there are dominant large patches within each unit, the formula is $\mathrm{LPI} = \frac{\max_{j=1}^{n}(a_{ij})}{A}(100)$, where n = number of patches in the landscape of patch type (class) i, $j = 1, \ldots, n$ patches, a_{ij} = area (m^2) of patch ij, A = Total landscape area.
	Area-weighted mean patch fractal dimension (AWMPED)	To calculate the complexity of patches shape within each unit. the formula is $\mathrm{AWMPED} = \sum_{j=1}^{n}\left[\left(\frac{21n(.25p_{ij})}{\ln a_{ij}}\right)\left(\frac{a_{ij}}{\sum_{j=1}^{n} a_{ij}}\right)\right]$, where m = number of patch types (classes) present in the landscape, n = number of patches in the landscape of patch type (class) $i, i = 1, \ldots, m$ or m patch types (classes), $j = 1, \ldots, n$ patches, p_{ij}= perimeter (m) of patch ij, a_{ij} = area (m^2) of patch ij.
	Shannon's diversity index (SHDI)	To evaluate the diversity of patches within each unit, the formula is $\mathrm{SHDI} = -\sum_{i=1}^{m}(P_i^{\circ} \ln P_i)$, where m = number of patch types (classes) present in the landscape, $i = 1, \ldots, m$ or m patch types (classes), P_i = proportion of the landscape occupied by patch type (class) i.
Land-use	Ratio of Urban Construction Land (RUL)	The proportion of urban and rural construction land, forests, and farmlands, which are the dominant land-use types in the study area.
	Ratio of Rural Construction Land (RRL)	
	Ratio of Forests (RF)	
	Ratio of Farmlands (RFL)	

3.3. Cluster of Landscape Character Types

K-Medoids clustering is an unsupervised classification method commonly used in machine learning. It can divide a given dataset into several groups with as little difference as possible within the same group. This method was applied to this study to identify and classify study units with similar landscape features. For a dataset containing N i-dimensional units, it needs to be classified into K groups, and the centroid of each group is O_K [17,18]. First, O_Ks were selected randomly among all samples, and the Euclidean distances from

the remaining points M to O_K were calculated one by one. In this step, the initial clusters were obtained by assigning Ms to the closest O_K based on the calculation results.

In the second step, K remaining points M were randomly selected to replace O_K, denoted as O_M, and the differences in distances from the remaining points to the centroid resulting from this behavior were calculated, denoted as C_{MK}. The total cost function T_{MK} was calculated to determine whether O_M, can replace the O_K, with the formula:

$$T_{MK} = \sum_{M=1}^{N} C_{MK} \tag{1}$$

A negative value of T_{MK} means that the total deviation decreases, and O_M replaces O_K as the new centroid. The above steps were iterated until T_{MK} no longer experienced changes.

Rationally determining the value of K is a key step toward making the clustering results meaningful. In this study, the Sum of Squared Error (SEE) curve and the classification results were combined to determine the K-value, with the aim being to reflect the critical characteristics of the study area with the fewest clusters while keeping the error within an acceptable range. The Partitioning Around Medoids (PAM) package was used to implement K-Medoids clustering in R. A total of 7878 units were used for clustering, covering three years 2000, 2020, and 2040, and each sample included three dimensions with 10 indicators altogether.

4. Results

4.1. Prediction of Land-Use Changes

We simulated the land-use data on the area for 2020 and used the Kappa coefficient to test the simulation results obtained using the PLUS model. The simulation results were compared with the status of the land space during 2020, and the Kappa coefficients and overall accuracy were calculated. Kappa coefficients were used to test the accuracy of the land-use prediction results. The Kappa coefficient ranged from 0 to 1, with a value greater than 0.7 indicating consistent and accurate prediction results [49]. The calculated overall accuracy was 90.2%, and the Kappa coefficient was 0.810, indicating a high degree of credibility. As shown in Table 4, during 2000–2020, 1039.24 km^2 of land-use conversion occurred. The largest proportion of land-use change is the conversion of farmlands to urban construction lands (64.8%), followed by the conversion of forests to farmlands (12.8%). The converted farmland is mainly located on the north bank of the river and west of the built-up areas. Large areas of forests in the southwest of the study area were converted to farmland (Figure 3). It is worth noting that the area of rural construction land increased by 18.4 km^2, while approximately 22.6 km^2 of rural construction land was converted into urban construction land.

From 2020 to 2040, the area of land-use change reached 727.03 km^2, with the change of land from farmland to urban construction areas accounting for 79.6% and 10.1% resulting from the conversion of forest to farmland (Table 5). Most of the farmlands within the central city have been converted into construction land, and the built-up areas have continually spread and grown. There has also been some expansion of urban construction land around some rivers and forest belts (Figure 3). Rural construction land has increased by 45.27 km^2, which is higher than the increase between 2000 and 2020. About 10.7 km^2 of rural construction land has been converted into urban construction land, which is lower than the decrease from 2000 to 2020 (Figure 4).

Table 4. Transfer matrix of land-use from 2000 to 2020.

		2000 (km^2)							
	Land-Use Types	Farmlands	Forests	Grasslands	Water Bodies	Urban Construction Lands	Rural Construction Lands	Other Lands	Total (2020)
2020 (km^2)	Farmlands	3707.18	132.82	2.16	8.20	2.94	2.50	0.16	3855.97
	Forests	67.68	1122.37	2.44	0.66	1.02	0.49	1.02	1195.69
	Grasslands	6.73	1.22	45.12	0.10	0.00	0.61	0.00	53.78
	Water bodies	26.27	1.65	0.33	143.12	0.83	0.58	0.15	172.94
	Urban Construction lands	673.10	31.24	0.35	5.54	266.52	22.64	0.03	999.43
	Rural Construction lands	38.59	2.90	0.02	0.38	3.34	54.09	0.00	99.32
	Other lands	0.18	0.01	0.00	0.30	0.04	0.00	2.52	3.05
	Total (2000)	4519.74	1292.22	50.42	158.30	274.70	80.92	3.89	6380.18

Table 5. Transfer matrix of land-use from 2020 to 2040.

		2020 (km^2)							
	Land-Use Types	Farmlands	Forests	Grasslands	Water Bodies	Urban Construction Lands	Rural Construction Lands	Other Lands	Total (2020)
2040 (km^2)	Farmlands	3253.27	73.64	18.80	0.00	0.00	0.00	0.13	3345.84
	Forests	0.00	1104.23	0.45	0.00	0.00	0.00	0.04	1104.72
	Grasslands	0.00	0.30	32.06	0.00	0.00	0.00	0.00	32.36
	Water bodies	0.00	0.00	0.00	172.94	0.00	0.00	0.00	172.94
	Urban Construction lands	578.35	16.18	2.15	0.00	999.43	10.72	0.26	1607.10
	Rural Construction lands	24.35	1.33	0.31	0.00	0.00	88.60	0.00	114.59
	Other lands	0.00	0.00	0.00	0.00	0.00	0.00	2.62	2.62
	Total (2020)	3855.97	1195.69	53.78	172.94	999.43	99.32	3.05	6380.18

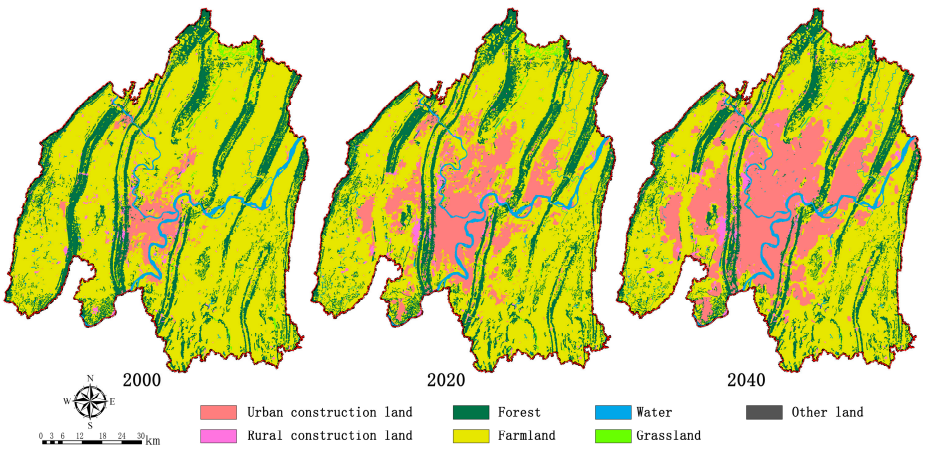

Figure 3. Land-use in 2000, 2020, and 2040.

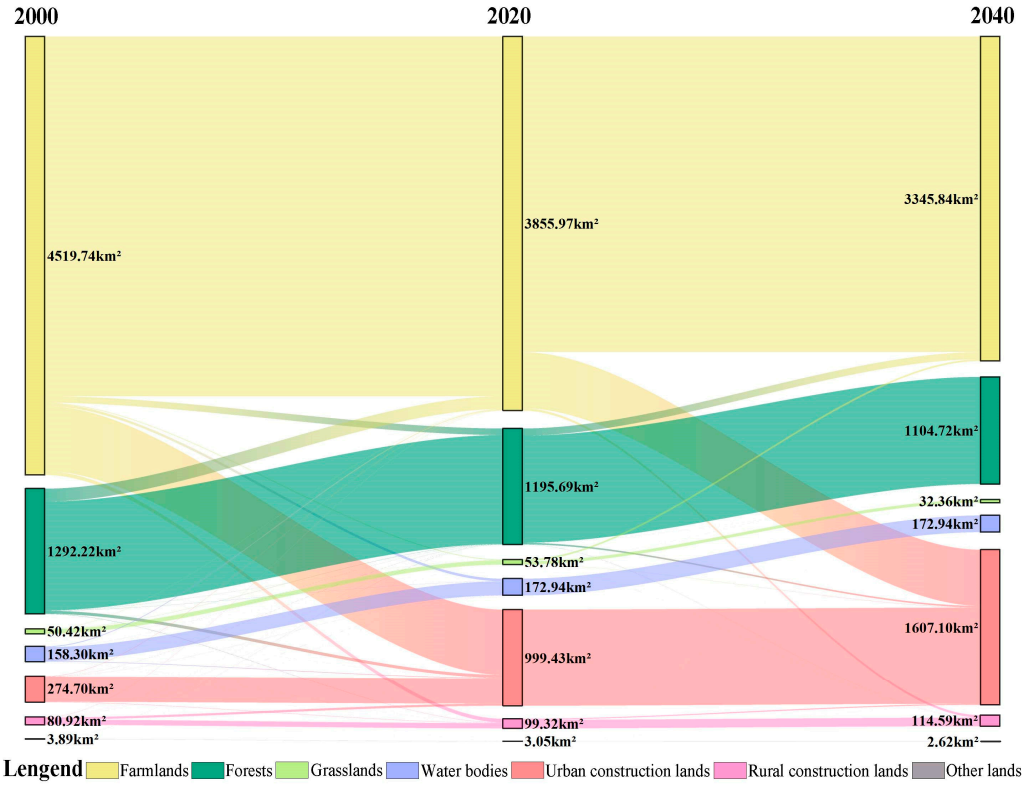

Figure 4. Sankey diagram for comparison of land-use dynamics in two-time intervals defined by three land-use maps for the years 2000, 2020 and 2040.

4.2. Cluster of Landscape Character Types

The SEE curve showed that after $K > 3$, the curve tended to flatten and the errors are acceptable (Figure 5). However, only three groups were unable to demonstrate the complex landscape characteristics of the study area. We tested three to nine groups one by one and found that when K was less than 7, the integrated landscape characteristics of construction and ecological spaces in urban fringe regions were neglected. However, if there were too many clusters, there would be information redundancy.

After multiple attempts, it was determined that the characteristics of each group were differentiated with minimal redundant information when $K = 8$. The characteristics of each type are shown in Figure 6. Types 1, 3, and 4 are all dominated by farmland. Type 1 can be characterized as transitional areas between agricultural and ecological spaces, with a higher forest proportion and patch diversity. Samples in Type 3 are dominated by farmlands, as evidenced by their relatively high LPI mean value. The values of various indicators for Type 4 are between those of Types 1 and 3. Types 2 and 6 have a high proportion of forests and significant variations in topography. Among them, samples in Type 6 are dominated by forest patches and have a higher ecological value, while Type 2 is composed of transitional areas between forests and farmlands, with both productive and ecological value. Compared to the other types, Types 5, 7, and 8 are characterized by the presence of construction land and relatively flat terrain. Most of the samples in Type 5 are distributed in the urban fringe area, with a higher proportion of forests and farmlands compared to other types. The samples in Type 8 are distributed in densely built-up areas, with strong patch dominance, regular shape, and low diversity, indicating the dominance of urban construction lands. Type 7 samples are distributed in the transition areas between Types 5 and 8. Type 7 also contains a certain amount of forests and farmlands, as well as a relatively high diversity of land patches.

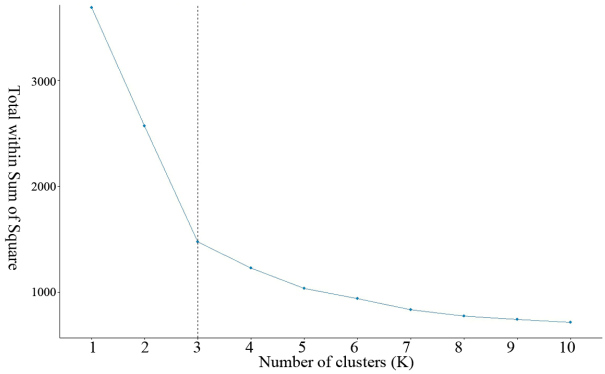

Figure 5. SEE curves for different Ks when clustering.

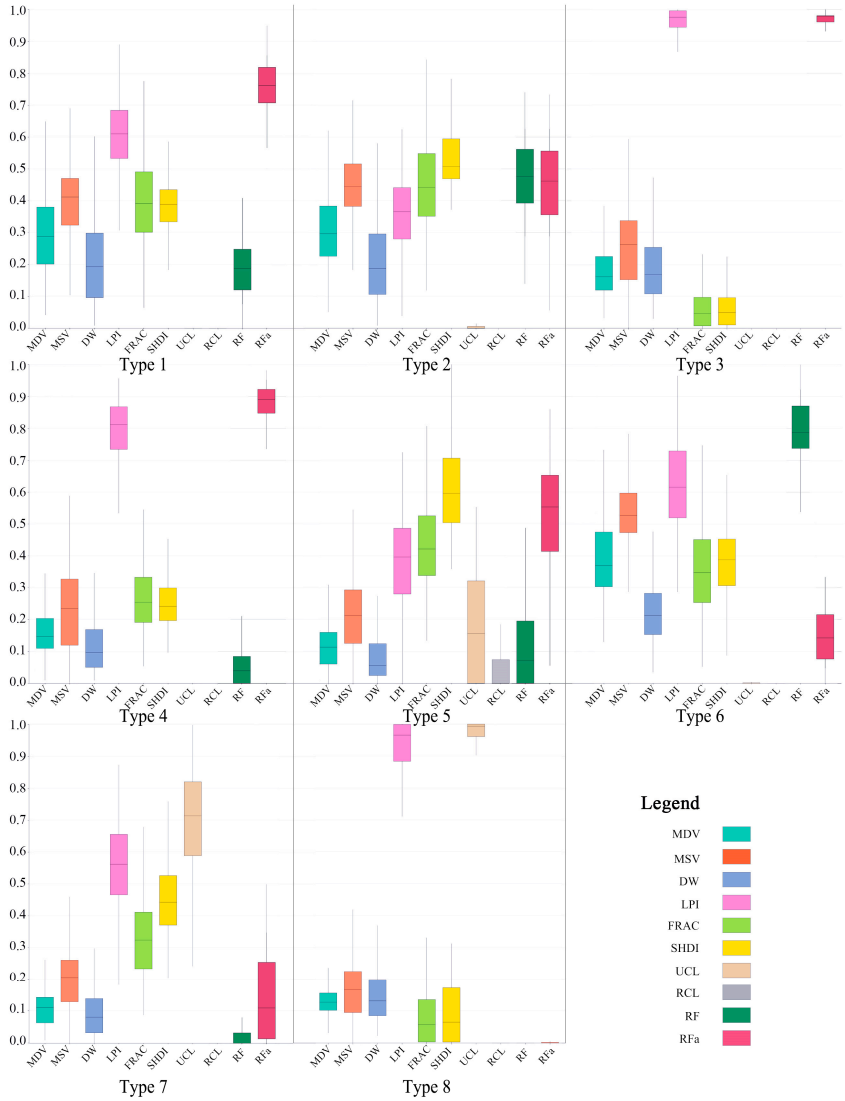

Figure 6. Cluster results of LCTs.

4.3. Spatial Distribution and Changes of Landscape Character Types

During the simulation for 2000–2040, the number and spatial distribution of the LCTs changed significantly (Figure 7). Table 6 shows that the samples of Types 1, 2, and 8 remain nearly unchanged from 2000 to 2020. The spatial distribution of Types 7 and 8, which are mainly urban construction land, shows an expansion from the densely built-up area to the suburbs. Type 7 is converted mainly to Type 8 (56%). Type 8 possesses a 100%

non-conversion rate, although the number is low, with only 14 study units. Samples in Type 3, which are dominated by farmlands, are converted to Types 4, 5, and 7, mainly in regions with flatter terrain. Type 4, located in the hills, is changed to Type 5 by 23.51%, mainly in the southeast and southwest of the study area. Simultaneously, 24.62% of the samples in Type 5 (containing significant rural construction land) are converted to Type 7, distributed between densely built-up areas and suburbs. Compared to the other LCTs, the conversion rate from Type 6 to Types 2, 3, and 4 is essentially the same, accounting for 5–7%.

The transfer matrix from 2020 to 2040 reveals that Types 1, 2, and 8 are the types with the least amount of change in sample numbers, with a limited number being converted to Type 1 and Type 5 (Table 7). There is a tendency for Types 7 and 8 to expand further into the periphery of the central city. The samples in Type 7 are only converted to Type 8. Types 3 and 4, distributed in the plains, and Type 6, with montane forests as the dominant cover, all have an increase in their non-conversion rate. They are mainly converted to Types 2, 4, and 5, which are the areas adjacent to the urban construction land. In contrast, the non-conversion rate of Type 5, located in the urban-rural transition zone, shows a decreasing trend. The probability of conversion to Type 7 is 42.05%, almost as high as the probability of maintaining the same type (45.13%).

According to the Sankey diagram of LCT changes (Figure 8), the most identifiable trends are the encroachment of farmland in the urban periphery by construction land (Types 3, 4, and 5 to Types 7 and 8) and the expansion of villages away from the densely built-up area (Types 1 and 4 to Type 5). The number of samples in Type 3 shows the largest decrease among the 8 types, from 852 to 430 (2000–2020). However, the decline in the number of samples in Type 3 slows down from 2020 to 2040 (326 in 2040). Meanwhile, 95 of Type 4 become Type 5, and 164 of Type 5 become Type 7. The number of Types 7 and 8 increased from 96 and 14 (in 2000), respectively, to 335 and 336 (in 2040). It is noteworthy that the number of Type 5 grows significantly from 2000 to 2020 (195 to 390), and few changes occur from 2020 to 2040, while nearly half of the samples come from the other types (mainly Types 1 and 4).

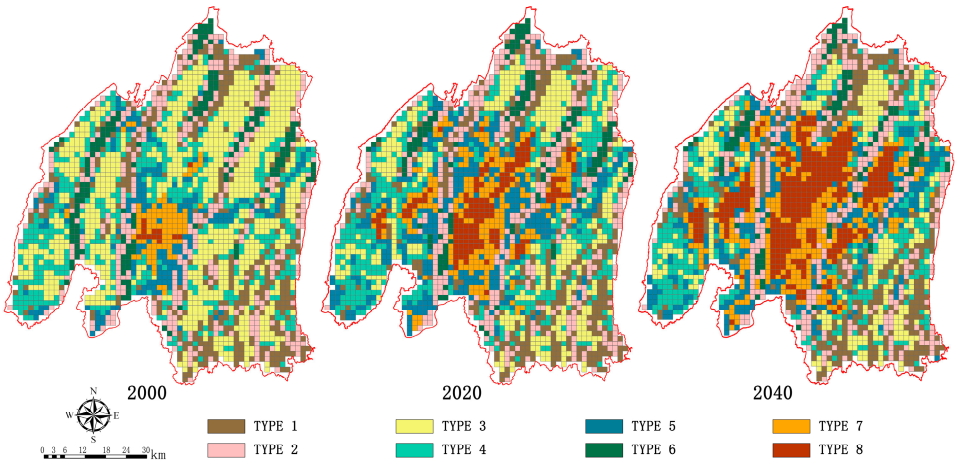

Figure 7. Spatial distribution of LCT in 2000, 2020, and 2040.

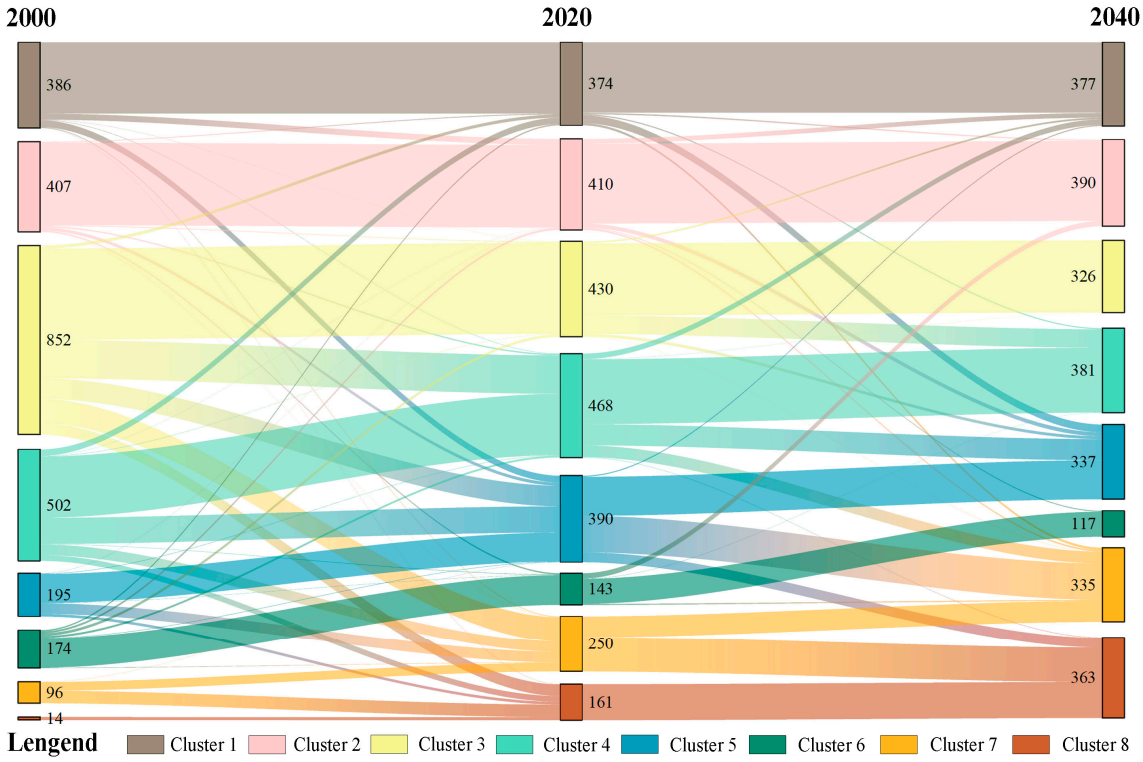

Figure 8. Sankey diagram for the comparison of LCTs in two-time intervals defined by three LCT maps for the years 2000, 2020 and 2040.

Table 6. Transfer matrix of LCTs from 2000 to 2020.

		2020 (The Proportion of Changes in Study Units %)							
	Type	1	2	3	4	5	6	7	8
2000 (%)	1	83.16	6.99	0.26	0.52	8.03	0.00	0.78	0.26
	2	0.98	91.40	0.98	1.47	3.44	1.47	0.25	0.00
	3	1.64	0.00	48.24	20.31	10.92	0.00	12.79	6.10
	4	5.78	0.20	0.40	54.98	23.51	0.40	9.56	5.18
	5	0.00	0.51	0.00	1.03	67.18	0.51	24.62	6.15
	6	3.45	5.17	6.90	5.17	1.15	77.01	1.15	0.00
	7	0.00	0.00	0.00	0.00	1.79	0.00	42.21	56.00
	8	0.00	0.00	0.00	0.00	0.00	0.00	0.00	100

Table 7. Transfer matrix of LCTs from 2020 to 2040.

		2040 (The Proportion of Changes in Study Units %)							
	Type	1	2	3	4	5	6	7	8
2020 (%)	1	85.03	1.60	0.00	1.34	9.36	0.00	2.67	0.00
	2	5.12	87.80	0.00	0.00	4.39	0.98	1.71	0.00
	3	1.86	0.00	75.58	19.30	3.02	0.00	0.23	0.00
	4	5.34	0.00	0.21	62.39	20.30	0.00	11.32	0.43
	5	1.28	0.00	0.00	0.00	45.13	0.00	42.05	11.54
	6	0.00	16.78	0.00	0.00	0.00	79.02	3.50	0.00
	7	0.00	0.00	0.00	0.00	0.00	0.00	38.00	62.00
	8	0.00	0.00	0.00	0.00	0.00	0.00	0.00	100

4.4. Contribution of the Driving Factors to Landscape Character Types Change

Figure 9a shows the contribution of each driving factor to the land-use conversion, with nighttime light being the largest contributor. It contributes 23.6%, 30.5%, 36.9%, 23.6%, and 21.5% to the conversion of farmland, forest, grassland, urban construction land, and rural construction land, respectively (Figure 9a). Elevation and POI density contribute 14.5% and 11.5%, respectively, in the conversion of farmland to the remaining land-use types. Similarly, the mean elevation and distance to trunk roads play a significant role in forest conversion, with contributions of 11.9% and 11.6%, respectively. The contribution of POI density to grassland conversion is much larger, standing at 16.9%. In contrast, the distance to water bodies has a dominant influence on the conversion of water bodies and urban construction land, with a contribution of 77.2% and 22.9%. Population density and distance to trunk roads contribute 15% and 13.1%, respectively, to the conversion of rural construction land.

Based on the driving factors' contribution to the change in LCTs, nighttime light and elevation have the most significant effect (Figure 9b). Specifically, the nighttime light has the highest contribution to Types 1, 4, 5, 7, and 8, with respective contributions of 22.7%, 28.1%, 21.4%, 26.3%, and 27.8%. Meanwhile, the elevation has the highest contribution to Types 3 and 6 (37.7% and 36.6%, respectively).

However, there are differences in the contribution of the driving factors to each LCT change. For Types 1 and 4, the driving factors with the largest impact are elevation and population density. For Type 2, the slope is the largest contributor (22.6%). Distance to trunk roads and distance to motorways also contribute 16.5% and 12.6%, respectively, which is similar to Type 3 (distance to trunk roads contributes 13.8%). For Types 5 and 8, the socio-economic factors of POI density and population density are the ones that contribute most to the types change (21.2% and 12.7% in Type 5, 16.8% and 13.7% in Type 8). For Type 7, the natural and socio-economic factors (POI density and distance to water bodies) contribute significantly to the type change, with 14.6% and 11.5%, respectively. It is noteworthy that slope and population density, with 14.1% and 12.3%, respectively, are the factors that contribute most to the change in Type 6.

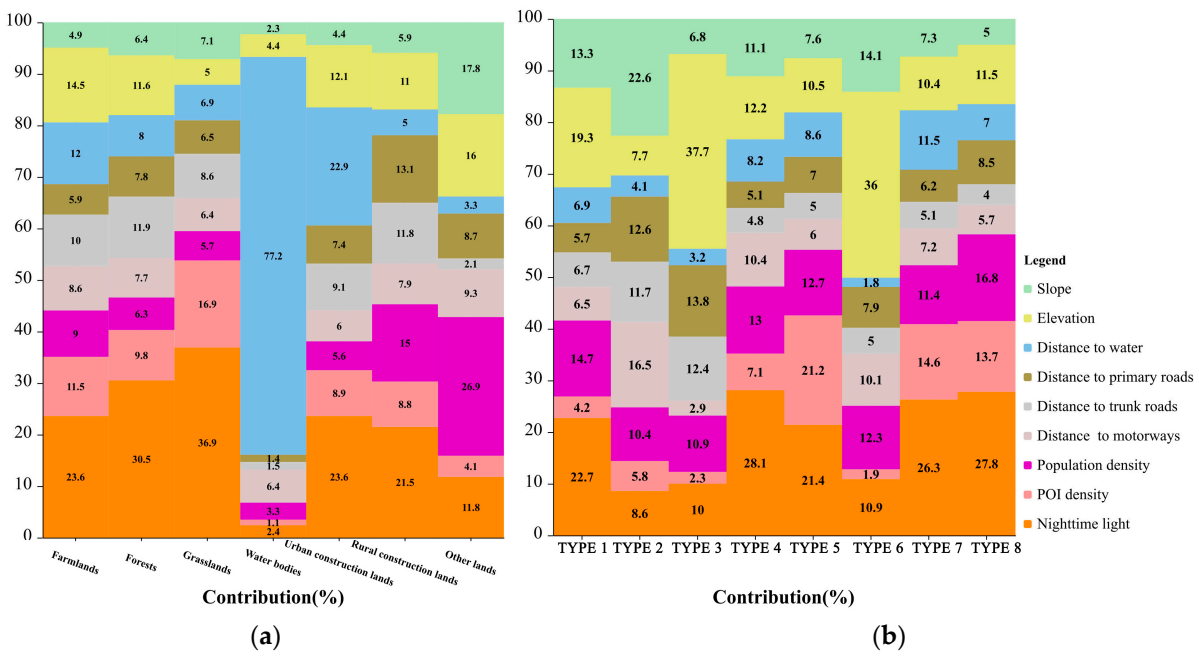

Figure 9. Contribution of the driving factors to (**a**) land-use conversion, and (**b**) LCT change.

5. Discussion

5.1. Advantages of Landscape Character Types for Landscape Management

Analyzing land-use change is often considered an intuitive method for understanding landscape changes during the urban development process. However, the characteristics of landscape spaces and their ecosystem service capacity are not only determined by land-use types but also influenced by the pattern and combination of ecological patches and terrain features. For example, numerous studies have demonstrated that a landscape's spatial pattern significantly impacts its structure and function [50]. Fragmented landscapes may impede the provision of ecosystem services, such as biodiversity conservation and climate change mitigation. Therefore, analyzing the evolution of urban landscapes from a composite perspective of LCTs can supplement land-use change analysis. Furthermore, it can reveal the potential ecological risks and changes in ecosystem service capacity brought about by land-use changes, which may manifest in different dimensions, such as the aggravation of ecological risks, decrease in supply levels, or variations in landscape perception.

Compared to analyzing only changes in land-use, considering changes in LCTs can better support spatial planning [22]. The classification of LCTs is inherently site-specific, as it often depends on attributes that imbue the study area with landscape identity and a sense of place, and highlight its unique qualities [51,52]. This suggests that the landscape characterization approach and the indicators used may vary depending on the specific landscape characters [53]. In this study, an indicator system was used to identify LCTs in the study area, which is a commonly used method. The index system covered three aspects: topography, landscape pattern, and land-use. The complex topography and water bodies in Chongqing characterized the engineering difficulties which need to be overcome during urban expansion. The landscape pattern indicators focused on the diversity, dominance, and fragmentation degree of patches, while the land-use indicators provided information on patch types. The LCTs and their changes identified were based on the indicator system having multiple meanings, which were enough to describe the landscape character changes brought about by urban construction land expansion in the study area during urbanization.

Identifying LCTs with strong local characteristics can be challenging to generalize, and traditional methods may lack adaptability. However, parametric methods can effectively address this issue [51]. Based on the indicator system, this approach can draw thematic maps for conveying specific information. Furthermore, by combining different thematic maps, diverse LCTs can be recognized [54]. Unsupervised clustering methods in machine learning provide a way to combine thematic maps of LCTs. By analyzing the intrinsic data features, subjective bias can be eliminated and more objective and unified classification criteria can be obtained [55]. The K-Medoids method used in this study can achieve LCTs classification independent of researchers and planning practitioners, and has strong interpretability, demonstrating the usability and value of the methods and indicators.

5.2. Relationships between Land-Use and Changes in Landscape Character Types

Over the past 20 years, the landscape character of the central city of Chongqing has changed significantly. These changes were closely related to land-use and have a great impact on the prediction of land-use in the next 20 years.

The most striking changes over the period from 2000 to 2040 were those from Type 3 (dominated by the farmland) and Type 5 (located in the urban-rural transition zone) to Types 7 and 8 (dominated by the construction land). Type 7 changed to Type 8 more than 50% of the time, which has a higher FRAC and SHDI with a lower LPI. This LCT change, caused by the expansion of construction land, is in line with the general pattern of urban development, especially the conversion of farmland into construction land [56,57]. During this period, the LPI of Type 3 decreases and the FRAC increases, implying that the original landscape pattern begins to be fragmented. The study units where the LCT changes occur are less numerous when farther away from the built-up area, which is the change of LCTs in the urban-rural gradient [58]. In contrast to Type 3, Type 5, as a category adjacent to built-up areas (where the forest, farmland, and construction land coexist), shows a decrease

in FRAC and SHDI during the change process, which can be explained by the change from originally diverse and fragmented farmland and forest to intact urban construction land [59].

From 2000 to 2020, the changing rate of Type 3 to Type 4 and 5 (31.23%) is much larger than that of Type 7 and 8 (18.89%). This phenomenon has been closely related to the strict implementation of the policy of "returning farmland to the forest" and "balance of farmland acquisition and compensation" in the study area [60]. Reasonable policy measures can effectively slow down the rate of construction land encroachment on farmland. It should be noted that although this is the relationship between LCTs and land-use found in Chongqing, it could be equally significant in the other urban regions [58,61].

Compared with the period of 2000 to 2020, the primary difference between 2020 and 2040 is a 42.05% change from Type 5 to Type 7. No significant increase or decrease in the number of Types 3, 4, and 5 occurs, which is likely to be caused by the gradual reduction in the area of suitable land for building as construction land expands [62] or the continued growth of the urban low-income population in the study area, most of whom cannot afford the housing loans located in the central city [63]. With economic development and capital accumulation, Types 7 and 8 have reached their ultimate capacity within the study area, and the rural population can purchase expensive housing in the central city, as evidenced by the decline in the number of Type 5 from 2020 to 2040.

Furthermore, Types 1, 2, and 6, did not change significantly in number from 2000 to 2040. Compared to areas with a gentle topography and low ecological value, such as Types 3 and 4, Type 1 has a richer ecosystem and is mostly distributed between cultivated and forested land, away from the central city, where there is little disturbance from human activities [64]. Types 2 and 6 have a larger topographic relief and a higher proportion of woodlands. Thus, as a result of the limitations posed by the topography of Chongqing's parallel mountain ranges, none of these three types are preferable for development, indicating that the complex topography and the protection of high- value ecological space will affect the expansion of construction land [65,66].

5.3. Influence of the Critical Driving Factors

Land-use and LCT change are influenced by a combination of natural, socio-economic, and transport accessibility factors [67]. In the central city of Chongqing, elevation is the most significant natural factor affecting change, which represents a substantial conversion from Type 3 to Types 4, 5, 7, and 8 from 2000 to 2020. It highlights the key role of natural factors in mountain cities for the change from one LCT (dominated by farmland) to another LCT (dominated by urban construction land), where the rapid development of the central city is reflected in the full use of the topography and the extension of roads. These findings are consistent with previous research by [68]. Distance to water bodies is another natural factor influencing the growth of urban construction land. Riverside locations are more accessible than inland ones, with easy-to-reach supplies such as drinking water [69].

This study reveals that socio-economic factors have a greater impact on the majority of LCTs (Types 1, 4, 5, 7, and 8). It indicates that economic development and urbanization play a critical role in landscape character changes, which is consistent with previous research [70]. Nighttime light is also identified as a significant factor influencing the growth of urban and rural construction land, and its impact on change in farmlands, forests, and grasslands is also noteworthy. The expansion of the urban construction land in central cities will cause a trend of decreasing farmland, which will continue till 2040.

Based on the phenomenon of more types (Types 5 and 7) located in the transition area between the densely built-up area and countryside change to urban construction lands (Type 8), this study finds that the entire central city has become much simpler in morphology. This implies a significant reduction in the diversity of landscape characters and an increase in ecological threats to urban construction land. Meanwhile, population density and POI density have a stronger impact on the above LCTs than on the other types,

suggesting that an increasing population and industrial agglomeration have raised the demand for higher-density urban space.

Hence, in future urban planning, population and POI densities in local areas (e.g., LCTs with high forest cover) should be controlled based on monitoring the encroachment of urban construction land on the surrounding farmland. The protection of river ecosystems is equally important and is integrated into urban planning. In addition, the periphery of urban construction land, as a target for potential population concentrations and rapid development traffic, is the most sensitive area in the process of urban expansion [71]. It should protect the prime farmlands located in these areas, improve accessibility to rural building sites, and promote sustainable rural development [72].

6. Conclusions

In this study, based on the location and landscape characteristics of the central city of Chongqing, nine influencing factors were selected from three aspects: nature, socio-economics, and transportation. The PLUS model was used to predict land-use in 2040. Based on the prediction results, the land-use in 2000, 2020, and 2040 was divided into 1.5 × 1.5 km study units. This way, the study units were clustered by nine indicators in three dimensions: topography, landscape pattern, and land-use features. Finally, the change in LCTs over the three years and their driving factors were clarified.

The results are as follows:

(1) If the urban development trend from 2000 to 2020 continues until 2040, urban construction land in the central city of Chongqing will encroach on a large amount of farmland (79.6%) and a small amount of forest (10.1%). There has also been some expansion of urban construction land around some rivers and forests.
(2) From 2000 to 2040, there is an encroachment of the LCTs (dominated by farmland) around the built-up area by another LCT (dominated by urban construction land), as well as an expansion of villages away from the built-up area.
(3) The driving factors contribute to the conversion of all land-use types, from high to low: the nighttime light, POI, elevation, and distance to trunk roads. The distance to water bodies mainly influences the conversion of water bodies and urban construction land. Population density and distance to trunk roads mainly influence the conversion of rural construction land.
(4) There are also differences in the main driving factors affecting changes in LCTs. The nighttime light has the highest contribution to Types 1, 4, 5, 7, and 8. The elevation has the highest contribution to Types 3 and 6.

The PLUS model is used to predict land-use and perform clustering as a basis for analyzing the spatial distribution of LCTs and the driving factors behind their changes. It has significant implications for urban planners and policy-makers to make proper judgments. Especially amongst the global trend of advocating sustainable urban development, the results of predicted land-use and LCTs can provide a scientific and accurate planning basis for the study area. The methods of this study are widely applicable to cities in different locations and can be further integrated with local policies for the clustering of LCTs and spatial planning.

Author Contributions: Conceptualization, Z.C. and J.H.; methodology, Z.C. and J.H.; software, Z.C. and J.M.; validation, Z.C. and J.H.; formal analysis, J.M.; investigation, J.M.; resources, J.H.; data curation, J.H.; writing—original draft preparation, J.M.; writing—review and editing, J.M.; visualization, J.M.; supervision, J.H.; project administration, J.H. All authors have read and agreed to the published version of the manuscript.

Funding: This research received no external funding.

Data Availability Statement: The data presented in this study are available on request from the corresponding author. The data are not publicly available due to the title assessment of authors.

Conflicts of Interest: The authors declare no conflict of interest.

References

1. Grimm, N.B.; Faeth, S.H.; Golubiewski, N.E.; Redman, C.L.; Wu, J.; Bai, X.; Briggs, J.M. Global change and the ecology of cities. *Science* **2008**, *319*, 756–760. [CrossRef]
2. Dolejš, M.; Nádvorník, J.; Raška, P.; Riezner, J. Frozen Histories or Narratives of Change? Contextualizing Land-Use Dynamics for Conservation of Historical Rural Landscapes. *Environ. Manag.* **2019**, *63*, 352–365. [CrossRef] [PubMed]
3. United Nations Population Division. *The World at Six Billion*; United Nations Secretariat: Washington, DC, USA, 2000; Volume 26, p. 841.
4. Cao, Y.; Bai, Z.; Zhou, W.; Ai, G. Gradient Analysis of Urban Construction Land Expansion in the Chongqing Urban Area of China. *J. Urban Plan. Dev.* **2015**, *141*, 05014009. [CrossRef]
5. Xie, Y.; Fang, C.; Lin, G.C.S.; Gong, H.; Qiao, B. Tempo-spatial patterns of land use changes and urban development in globalizing China: A study of Beijing. *Sensors* **2007**, *7*, 2881–2906. [CrossRef]
6. Gong, J.; Yang, J.; Tang, W. Spatially Explicit Landscape-Level Ecological Risks Induced by Land Use and Land Cover Change in a National Ecologically Representative Region in China. *Int. J. Environ. Res. Public Health* **2015**, *12*, 14192–14215. [CrossRef] [PubMed]
7. Jin, X.; Jin, Y.; Mao, X. Ecological risk assessment of cities on the Tibetan Plateau based on land use/land cover changes—Case study of Delingha City. *Ecol. Indic.* **2019**, *101*, 185–191. [CrossRef]
8. Sala, O.E.; Chapin, F.R.; Armesto, J.J.; Berlow, E.; Bloomfield, J.; Dirzo, R.; Huber-Sanwald, E.; Huenneke, L.F.; Jackson, R.B.; Kinzig, A.; et al. Global biodiversity scenarios for the year 2100. *Science* **2000**, *287*, 1770–1774. [CrossRef]
9. Xie, H.; Wang, P.; Huang, H. Ecological risk assessment of land use change in the Poyang Lake Eco-economic Zone, China. *Int. J. Environ. Res. Public Health* **2013**, *10*, 328–346. [CrossRef]
10. She, Y.; Shen, L.; Jiao, L.; Zuo, J.; Tam, V.W.Y.; Yan, H. Constraints to achieve infrastructure sustainability for mountainous townships in China. *Habitat Int.* **2018**, *73*, 65–78. [CrossRef]
11. Karpouzoglou, T.; Dewulf, A.; Perez, K.; Gurung, P.; Regmi, S.; Isaeva, A.; Foggin, M.; Bastiaensen, J.; Van Hecken, G.; Zulkafli, Z.; et al. From present to future development pathways in fragile mountain landscapes. *Environ. Sci. Policy* **2020**, *114*, 606–613. [CrossRef]
12. Lin, X.; Wang, Z. Landscape ecological risk assessment and its driving factors of multi-mountainous city. *Ecol. Indic.* **2023**, *146*, 109823. [CrossRef]
13. Yao, F.; Hao, C.; Zhang, J. Simulating urban growth processes by integrating cellular automata model and artificial optimization in Binhai New Area of Tianjin, China. *Geocarto Int.* **2016**, *31*, 612–627. [CrossRef]
14. Molinero-Parejo, R.; Aguilera-Benavente, F.; Gómez-Delgado, M.; Shurupov, N. Combining a land parcel cellular automata (LP-CA) model with participatory approaches in the simulation of disruptive future scenarios of urban land use change. *Comput. Environ. Urban Syst.* **2023**, *99*, 101895. [CrossRef]
15. Zhang, Y.; Chang, X.; Liu, Y.F.; Lu, Y.C.; Wang, Y.H.; Liu, Y.L. Urban expansion simulation under constraint of multiple ecosystem services (MESs) based on cellular automata (CA)-Markov model: Scenario analysis and policy implications. *Land Use Policy* **2021**, *108*, 105667. [CrossRef]
16. Okwuashi, O.; Ndehedehe, C.E. Integrating machine learning with Markov chain and cellular automata models for modelling urban land use change. *Remote Sens. Appl. Soc. Environ.* **2021**, *21*, 100461. [CrossRef]
17. Lemonsu, A.; Viguié, V.; Daniel, M.; Masson, V. Vulnerability to heat waves: Impact of urban expansion scenarios on urban heat island and heat stress in Paris (France). *Urban Clim.* **2015**, *14*, 586–605. [CrossRef]
18. Rifat, S.A.A.; Liu, W. Predicting future urban growth scenarios and potential urban flood exposure using Artificial Neural Network-Markov Chain model in Miami Metropolitan Area. *Land Use Policy* **2022**, *114*, 105994. [CrossRef]
19. Wu, J. Landscape sustainability science (II): Core questions and key approaches. *Landsc. Ecol.* **2021**, *36*, 2453–2485. [CrossRef]
20. Turetta, A.P.D.; Prado, R.B.; Valladares, G.D.S. Evaluating the Potential of Landscape Metrics in Supporting Landscape Planning in Atlantic Forest: Rio de Janeiro, Brazil. *Int. J. Agric. Environ.* **2013**, *4*, 55–67. [CrossRef]
21. Karasov, O.; Külvik, M.; Burdun, I. Deconstructing landscape pattern: Applications of remote sensing to physiognomic landscape mapping. *Geojournal* **2021**, *86*, 529–555. [CrossRef]
22. Kim, K.; Pauleit, S. Landscape character, biodiversity and land use planning: The case of Kwangju City Region, South Korea. *Land Use Policy* **2007**, *24*, 264–274. [CrossRef]
23. Swanwick, C. Society's attitudes to and preferences for land and landscape. *Land Use Policy* **2009**, *26*, S62–S75. [CrossRef]
24. Liu, W.; Yu, Z. Identification and assessment of landscape character of Haidian District, Beijing. *Chin. J. Ecol.* **2016**, *35*, 1338–1344. [CrossRef]
25. Ode, Å.; Tveit, M.S.; Fry, G. Capturing Landscape Visual Character Using Indicators: Touching Base with Landscape Aesthetic Theory. *Landsc. Res.* **2008**, *33*, 89–117. [CrossRef]
26. Meng, Y.; Xing, H. Exploring the relationship between landscape characteristics and urban vibrancy: A case study using morphology and review data. *Cities* **2019**, *95*, 102389. [CrossRef]
27. Bartlett, D.; Gomez-Martin, E.; Milliken, S.; Parmer, D. Introducing landscape character assessment and the ecosystem service approach to India: A case study. *Landsc. Urban Plan.* **2017**, *167*, 257–266. [CrossRef]

28. Medeiros, A.; Fernandes, C.; Gonçalves, J.F.; Farinha-Marques, P. A diagnostic framework for assessing land-use change impacts on landscape pattern and character—A case-study from the Douro region, Portugal. *Landsc. Urban Plan.* **2022**, *228*, 104580. [CrossRef]
29. Liu, X.; Ming, Y.; Liu, Y.; Yue, W.; Han, G. Influences of landform and urban form factors on urban heat island: Comparative case study between Chengdu and Chongqing. *Sci. Total Environ.* **2022**, *820*, 153395. [CrossRef] [PubMed]
30. Xiang, S.; Wang, Y.; Deng, H.; Yang, C.; Wang, Z.; Gao, M. Response and multi-scenario prediction of carbon storage to land use/cover change in the main urban area of Chongqing, China. *Ecol. Indic.* **2022**, *142*, 109205. [CrossRef]
31. Li, W.; Wang, Y.; Xie, S.; Cheng, X. Coupling coordination analysis and spatiotemporal heterogeneity between urbanization and ecosystem health in Chongqing municipality, China. *Sci. Total Environ.* **2021**, *791*, 148311. [CrossRef]
32. Zhang, Q.; Chen, C.; Wang, J.; Yang, D.; Zhang, Y.; Wang, Z.; Gao, M. The spatial granularity effect, changing landscape patterns, and suitable landscape metrics in the Three Gorges Reservoir Area, 1995–2015. *Ecol. Indic.* **2020**, *114*, 106259. [CrossRef]
33. Chen, J.; Gao, M.; Cheng, S.; Hou, W.; Song, M.; Liu, X.; Liu, Y. Global 1 km × 1 km gridded revised real gross domestic product and electricity consumption during 1992–2019 based on calibrated nighttime light data. *Sci. Data* **2022**, *9*, 202. [CrossRef]
34. Gao, L.; Tao, F.; Liu, R.; Wang, Z.; Leng, H.; Zhou, T. Multi-scenario simulation and ecological risk analysis of land use based on the PLUS model: A case study of Nanjing. *Sustain. Cities Soc.* **2022**, *85*, 104055. [CrossRef]
35. Li, X.; Fu, J.; Jiang, D.; Lin, G.; Cao, C. Land use optimization in Ningbo City with a coupled GA and PLUS model. *J. Clean. Prod.* **2022**, *375*, 134004. [CrossRef]
36. Liang, X.; Guan, Q.; Clarke, K.C.; Liu, S.; Wang, B.; Yao, Y. Understanding the drivers of sustainable land expansion using a patch-generating land use simulation (PLUS) model: A case study in Wuhan, China. *Comput. Environ. Urban Syst.* **2021**, *85*, 101569. [CrossRef]
37. Zhang, X.; Jie, X.; Ning, S.; Wang, K.; Li, X. Coupling and coordinated development of urban land use economic efficiency and green manufacturing systems in the Chengdu-Chongqing Economic Circle. *Sustain. Cities Soc.* **2022**, *85*, 104012. [CrossRef]
38. Lu, D.; Wang, Y.; Yang, Q.; Wang, Z.; Lin, A.; Tang, Y.; Li, Y. Effects of population spatial redistribution on vegetation greenness: A case study of Chongqing, China. *Ecol. Indic.* **2022**, *138*, 108803. [CrossRef]
39. Nyanga, A.; Kessler, A.; Tenge, A. Key socio-economic factors influencing sustainable land management investments in the West Usambara Highlands, Tanzania. *Land Use Policy* **2016**, *51*, 260–266. [CrossRef]
40. Kikuchi, H.; Emberger, G.; Ishida, H.; Fukuda, A.; Kobayakawa, S. Dynamic simulations of compact city development to counter future population decline. *Cities* **2022**, *127*, 103753. [CrossRef]
41. Giles-Corti, B.; Saghapour, T.; Turrell, G.; Gunn, L.; Both, A.; Lowe, M.; Rozek, J.; Roberts, R.; Hooper, P.; Butt, A.; et al. Spatial and socioeconomic inequities in liveability in Australia's 21 largest cities: Does city size matter? *Health Place* **2022**, *78*, 102899. [CrossRef] [PubMed]
42. Wang, J.; Wu, K.; Du, Y. Does air pollution affect urban housing prices? Evidence from 285 Chinese prefecture-level cities. *J. Clean. Prod.* **2022**, *370*, 133480. [CrossRef]
43. Garriga, C.; Hedlund, A.; Tang, Y.; Wang, P. Rural-urban migration and house prices in China. *Reg. Sci. Urban Econ.* **2021**, *91*, 103613. [CrossRef]
44. Liu, G.; Wang, X.; Gu, J.; Liu, Y.; Zhou, T. Temporal and spatial effects of a 'Shan Shui' landscape on housing price: A case study of Chongqing, China. *Habitat Int.* **2019**, *94*, 102068. [CrossRef]
45. Kasraian, D.; Li, L.; Raghav, S.; Shalaby, A.; Miller, E.J. Regional transport accessibility and residential property values: The case study of the Greater Toronto and Hamilton area. *Case Stud. Transp. Policy* **2023**, *11*, 100932. [CrossRef]
46. Freiria, S.; Sousa, N.; Calvo-Poyo, F. Spatial analysis of the impact of transport accessibility on regional performance: A study for Europe. *J. Transp. Geogr.* **2022**, *102*, 103371. [CrossRef]
47. Winkler, K.; Fuchs, R.; Rounsevell, M.; Herold, M. Global land use changes are four times greater than previously estimated. *Nat. Commun.* **2021**, *12*, 2501. [CrossRef]
48. Cassin, J. Chapter 9—Nature-based solutions for source water protection in North America. In *Nature-Based Solutions and Water Security*; Cassin, J., Matthews, J.H., Gunn, E.L., Eds.; Elsevier: Amsterdam, The Netherlands, 2021; pp. 179–214.
49. Wu, C.; Chen, B.; Huang, X.; Dennis Wei, Y.H. Effect of land-use change and optimization on the ecosystem service values of Jiangsu province, China. *Ecol. Indic.* **2020**, *117*, 106507. [CrossRef]
50. Rudge, M.L.M.; Levick, S.R.; Bartolo, R.E.; Erskine, P.D. Developing landscape-scale forest restoration targets that embrace spatial pattern. *Landsc. Ecol.* **2022**, *37*, 1747–1760. [CrossRef]
51. Fry, G.; Tveit, M.S.; Ode, Å.; Velarde, M.D. The ecology of visual landscapes: Exploring the conceptual common ground of visual and ecological landscape indicators. *Ecol. Indic.* **2009**, *9*, 933–947. [CrossRef]
52. Atik, M.; Işıklı, R.C.; Ortaçeşme, V. Clusters of landscape characters as a way of communication in characterisation: A study from side, Turkey. *J. Environ. Manag.* **2016**, *182*, 385–396. [CrossRef]
53. Gormus, S.; Oğuz, D.; Eşbah TuNÇAY, H.; Cengiz, S. Using Landscape Character Analysis to Assess The Relationship Between Protected and Nonprotected Areas: The Case of The Küre Mountains National Park. *Tarım Bilim. Derg.* **2021**, *27*, 414–425. [CrossRef]
54. Lu, Y.; Xu, S.; Liu, S.; Wu, J. An approach to urban landscape character assessment: Linking urban big data and machine learning. *Sustain. Cities Soc.* **2022**, *83*, 103983. [CrossRef]

55. Chuman, T.; Romportl, D. Multivariate classification analysis of cultural landscapes: An example from the Czech Republic. *Landsc. Urban Plan.* **2010**, *98*, 200–209. [CrossRef]
56. Estoque, R.C.; Murayama, Y. Examining the potential impact of land use/cover changes on the ecosystem services of Baguio city, the Philippines: A scenario-based analysis. *Appl. Geogr.* **2012**, *35*, 316–326. [CrossRef]
57. Acheampong, M.; Yu, Q.; Enomah, L.D.; Anchang, J.; Eduful, M. Land use/cover change in Ghana's oil city: Assessing the impact of neoliberal economic policies and implications for sustainable development goal number one—A remote sensing and GIS approach. *Land Use Policy* **2018**, *73*, 373–384. [CrossRef]
58. Yang, D.; Zhang, P.; Jiang, L.; Zhang, Y.; Liu, Z.; Rong, T. Spatial change and scale dependence of built-up land expansion and landscape pattern evolution—Case study of affected area of the lower Yellow River. *Ecol. Indic.* **2022**, *141*, 109123. [CrossRef]
59. Dadashpoor, H.; Azizi, P.; Moghadasi, M. Land use change, urbanization, and change in landscape pattern in a metropolitan area. *Sci. Total Environ.* **2019**, *655*, 707–719. [CrossRef]
60. Zhang, H.; Wang, Z.; Chai, J. Land use\cover change and influencing factors inside the urban development boundary of different level cities: A case study in Hubei Province, China. *Heliyon* **2022**, *8*, e10408. [CrossRef]
61. Darvishi, A.; Yousefi, M.; Marull, J. Modelling landscape ecological assessments of land use and cover change scenarios. Application to the Bojnourd Metropolitan Area (NE Iran). *Land Use Policy* **2020**, *99*, 105098. [CrossRef]
62. Wolf, I.D.; Sobhani, P.; Esmaeilzadeh, H. Assessing Changes in Land Use/Land Cover and Ecological Risk to Conserve Protected Areas in Urban–Rural Contexts. *Land* **2023**, *12*, 231. [CrossRef]
63. Lerner, A.M.; Eakin, H.C.; Tellman, E.; Bausch, J.C.; Hernández Aguilar, B. Governing the gaps in water governance and land-use planning in a megacity: The example of hydrological risk in Mexico City. *Cities* **2018**, *83*, 61–70. [CrossRef]
64. Yang, Z.; Hong, Y.; Guo, Q.B.; Yu, X.X.; Zhao, M.S. The Impact of Topographic Relief on Population and Economy in the Southern Anhui Mountainous Area, China. *Sustainability* **2022**, *14*, 4332. [CrossRef]
65. Siddique, S.; Uddin, M.M. Green space dynamics in response to rapid urbanization: Patterns, transformations and topographic influence in Chattogram city, Bangladesh. *Land Use Policy* **2022**, *114*, 105974. [CrossRef]
66. Kiziridis, D.A.; Mastrogianni, A.; Pleniou, M.; Tsiftsis, S.; Xystrakis, F.; Tsiripidis, I. Simulating Future Land Use and Cover of a Mediterranean Mountainous Area: The Effect of Socioeconomic Demands and Climatic Changes. *Land* **2023**, *12*, 253. [CrossRef]
67. Marcucci, D.J. Landscape history as a planning tool. *Landsc. Urban Plan.* **2000**, *49*, 67–81. [CrossRef]
68. Jia, L.; Ma, Q.; Du, C.; Hu, G.; Shang, C. Rapid urbanization in a mountainous landscape: Patterns, drivers, and planning implications. *Landsc. Ecol.* **2020**, *35*, 2449–2469. [CrossRef]
69. Qu, W.Y.; Zhao, S.Q.; Sun, Y. Spatiotemporal patterns of urbanization over the past three decades: A comparison between two large cities in Southwest China. *Urban Ecosyst.* **2014**, *17*, 723–739. [CrossRef]
70. Wang, L.; Wu, L.; Zhang, W. Impacts of land use change on landscape patterns in mountain human settlement: The case study of Hantai District (Shaanxi, China). *J. Mt. Sci.* **2021**, *18*, 749–763. [CrossRef]
71. Xiu, N.; Ignatieva, M.; van den Bosch, C.K.; Zhang, S.; Sveriges, L. Applying a socio-ecological green network framework to Xi'an City, China. *Landsc. Ecol. Eng.* **2020**, *16*, 135–150. [CrossRef]
72. Sun, D.L.; Hong, B.T.; Ren, P. Spatiotemporal evolution and driving factors of the rural settlements in the mountain-plain transitional zone. *Int. J. Agric. Biol. Eng.* **2022**, *15*, 149–155. [CrossRef]